Collision Avoidance in Wireless Powered Sensor Networks with Backscatter Communications

Constantinos Psomas and Ioannis Krikidis
KIOS Research and Innovation Center of Excellence
Department of Electrical and Computer Engineering, University of Cyprus, Cyprus
e-mail: {psomas, krikidis}@ucy.ac.cy

***Abstract*—Wireless powered communications is a promising technology for next-generation low-powered sensor networks such as the Internet of Things. This paper deals with backscatter communications in sensor networks, an ideal technology for low-powered battery-less devices. However, in contrast to conventional communications, backscattering suffers from collisions due to multiple concurrent transmissions and from a dyadic backscatter channel, which greatly attenuates the received signal at the reader. We study a wireless backscatter communication network from a large-scale point-of-view, and consider various techniques to overcome these limitations such as antenna directionality, ultra-narrow band transmissions and successive interference cancellation. Using stochastic geometry tools, we derive mathematical expressions for the decoding probability and present the significant gains, which can be achieved from these techniques.**

***Index Terms*—Backscatter communications, sensor networks, ultra narrow band, Poisson point process.**

I. Introduction

The emergence of the notion referred to as the Internet of Things (IoT), has raised many questions regarding the sensors' energy requirements and energy consumption. The massive and ubiquitous deployment of sensor nodes will make it impractical or in some cases impossible, to individually recharge and/or manage these devices on a regular basis. Wireless power transfer (WPT), i.e. harvesting energy from electromagnetic radiation, is a practical and promising method for powering low-powered devices remotely and on-demand. Of significant interest, is the concept of wireless powered communications [1]. In this case, the transmitted/received signals are used not only for information but also for energy exchange. A wireless powered communication network (WPCN) refers to a network architecture, where the terminals power their uplink transmissions by harvesting energy from radio frequency (RF) signals, transmitted by a power beacon or an access point in a dedicated orthogonal channel [2]. This architecture is ideal for next-generation wireless sensor networks such as the IoT.

Most studies on WPT, focus on devices which harvest energy through a rectifying-antenna (rectenna), a diode-based circuit that converts RF signals to direct-current voltage [3]. Even though this approach is feasible, the amount of energy harvested via this operation is usually very small compared to the energy needed to power the device. Another well-known approach is backscatter communications [1], a technology used mainly for radio frequency identification (RFID) [4]. In this case, a part of the received signal is scattered back after it is modulated using a load modulation scheme [5]. Here, the energy consumption is very low since it requires just one RF chain for transmission/reception and most of its components are passive. In the literature, few studies exist on backscattering communication networks from a system level point-of-view. In [6], the performance of various anti-collision techniques is studied in backscatter sensor networks; the authors show that the modulation employed at each sensor is crucial to achieve adequate network performance. The work in [7] studies the performance of ultra high frequency RFID systems and present a 3D analytical model under cascaded fading channels; results for the detection probability of a tag and for the reliable reading range are provided. Finally, the work in [8] considers backscatter communication networks with multiple power beacons, where each beacon serves a cluster of devices; the performance of the network is studied in terms of the coverage probability and the capacity.

Apart from [8], related work on backscatter networks considers fixed and deterministic topologies. Moreover, [6] and [8] do not consider a dyadic backscatter channel, which is critical to the backscatter network's performance. Motivated by the above, in this paper, we study backscatter sensor networks with spatial randomness. We take into account the dyadic backscatter channel, i.e. two-way channel, in our analysis and consider the two extreme cases where the two channels are fully correlated and completely uncorrelated. Due to the existence of high interference levels (collisions) at the reader from multiple concurrent transmissions, we investigate three collision avoidance techniques to boost the performance. Specifically, we consider antenna directionality and successive interference cancellation (SIC) at the reader as well as ultra-narrow band transmissions from the sensors. We derive closed-form expressions for the decoding probability, i.e. the probability of decoding a random sensor, using mathematical tools from stochastic geometry. Our results show that a combination of these techniques is needed to achieve significant gains.

Notation: $\mathbb{P}(X)$ denotes the probability of the event X and $\mathbb{E}[X]$ represents the expected value of X, $\Re[x]$ and $\Im[x]$ are the real and imaginary parts of x, respectively, $\imath = \sqrt{-1}$ is the imaginary unit, $\Gamma(\alpha, x) = \int_x^\infty \exp\{-t\} t^{\alpha-1} \mathrm{d}t$ is the upper incomplete gamma function [9, 8.350.2] and $K_0(x)$ is the modified Bessel function of the second kind of order zero.

This work was supported by the Research Promotion Foundation, Cyprus under the project COM-MED with pr. no. KOINA/ERANETMED/1114/03.

978-1-5090-3009-5/17/$31.00 ©2017 IEEE

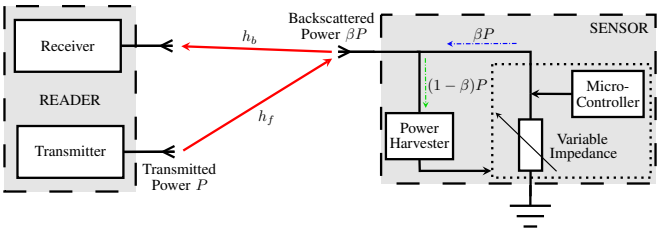

Fig. 1: Wireless powered backscatter communications.

II. System Model

A. Topology

We consider a single-cell WPCN utilizing a bandwidth BW with multiple randomly deployed sensors with backscatter communication capabilities. The coverage (reading) zone is modeled as a disc of radius ξ, where the reader is located at the origin of the disc with an exclusion zone of radius ζ around it with $\xi > \zeta \geq 1$. The exclusion zone defines the minimum reading distance between the reader and a sensor whereas ξ defines the maximum reading distance [4]; the restriction $\zeta \geq 1$ ensures the harvested energy is never greater than the transmitted power. The location of the sensors is modeled as a homogeneous Poisson point process (PPP) Ψ with intensity λ. Each sensor is equipped with a single antenna and a circuit responsible for modulating and transmitting back the information to the reader.

B. Channel model

We assume that all wireless links suffer from small-scale block fading and large-scale path-loss effects. A backscatter channel is dyadic, that is, it is characterized by a forward link (reader to sensor) and a backscatter link (sensor to reader). We denote by h_f^i and h_b^i the channel coefficients for the forward and backscatter link with the i-th sensor, respectively [5]; it's clear that the two links can be correlated by a coefficient ρ, $0 \leq \rho \leq 1$. The fading is considered to be Rayleigh distributed[1] so the power of the channel fading is an exponential random variable. Therefore, the probability distribution function (pdf) of the backscatter channel power is given by the pdf of the product of two exponential random variables. For the sake of analytical tractability, we consider the cases $\rho = 0$ (independent links) and $\rho = 1$ (perfectly correlated links). The pdf $f_h(h, \rho)$ of the i-th sensor's backscatter channel power $h_i = |h_f^i|^2 |h_b^i|^2$ where $|h_f^i|^2$ and $|h_b^i|^2$ have correlation ρ is

$$f_h(h, 0) = 2\mu_f \mu_b K_0 \left(2\sqrt{\mu_f \mu_b h}\right), \tag{1}$$

for uncorrelated channels, and

$$f_h(h, 1) = \frac{1}{2}\sqrt{\frac{\mu_f \mu_b}{h}} \exp\left\{-\sqrt{\mu_f \mu_b h}\right\}, \tag{2}$$

for perfectly correlated channels, where μ_f and μ_b are the rate parameters of $|h_f^i|^2$ and $|h_b^i|^2$, respectively; throughout this work we consider $\mu_f = \mu_b = 1$. The proofs for the above pdfs are omitted as they can be derived from the pdfs for the product of two Rayleigh random variables given in [5]. The path-loss model assumes that the received power is proportional to $d_i^{-\alpha}$ where d_i is the Euclidean distance from the origin to the i-th sensor and $\alpha > 1$ is the path-loss exponent. The pdf of the distance d_i is given by

$$f_d(x) = \frac{1}{\pi(\xi^2 - \zeta^2)}. \tag{3}$$

Finally, we assume that all wireless links exhibit additive white Gaussian noise with variance σ^2.

[1]Rayleigh is used for simplicity but without loss of generality, other channel models such as Rice and Nakagami could also be considered.

C. Backscatter communications

The reader transmits an unmodulated RF signal towards the sensors given by

$$s(t) = \sqrt{2P}\Re[\exp\{\imath 2\pi f t\}], \tag{4}$$

where $P = \mathbb{E}[s^2(t)]$ is the reader's transmit power and f denotes the carrier frequency. The received signal obtained by a sensor is modulated and reflected back to the reader [4]. We model the ratio of the received power reflected back by a sensor with a reflection coefficient $\beta \in [0, 1]$; this means βP is the backscattered power and $(1-\beta)P$ is used to power the load modulation scheme which varies the impedance between different states [4], [8]. The backscattered power highly depends on the received power, the impedance matching of the circuit and the energy needed to operate. Fig. 1 schematically depicts the considered backscatter communication scheme. The reader attempts to decode the signal from the i-th sensor given by

$$y_i(t) = \tilde{y}_i(t) + \sum_{j \neq i} \tilde{y}_j(t) + \Re[n(t)\exp\{\imath 2\pi f t)\}], \tag{5}$$

where $\tilde{y}_i(t) = \sqrt{2\beta P}|h_f^i||h_b^i|d_i^{-\alpha}\Re[x_i(t)\exp\{\imath(2\pi f t + \theta_f^i(t) + \theta_b^i(t))\}]$, $x_i(t)$ is a modulated energy signal from the i-th sensor with $\mathbb{E}[|x_i(t)|^2] = 1$, $\theta_f^i(t)$, $\theta_b^i(t)$ are the phase shifts and $n(t)$ is a circularly symmetric complex Gaussian random variable with zero mean and variance σ^2. Then, the signal-to-interference-plus-noise ratio (SINR) of the reader for the i-th sensor is

$$\gamma_i = \frac{\beta P h_i}{d_i^{2\alpha}(\sigma^2 + I_i)}, \tag{6}$$

where $I_i = \beta P \sum_{j \in \Psi \setminus \{i\}} \frac{h_j}{d_j^{2\alpha}}$. Note that the path-loss exponent is doubled as a result of the dyadic backscatter channel.

III. Collision Avoidance Techniques

The main issue in backscatter communication networks is the existence of collision (interference) at the reader, due to the simultaneous transmission from multiple sensors, which reduces the reader's ability to decode a sensor's signal. To decrease these negative effects, numerous techniques have been proposed to detect and avoid such collisions [4]. In this work, we investigate the following techniques.

1) Sectorized directional antennas: The reader is equipped with D sectorized directional antennas, i.e. the beamwidth of the antenna is $\frac{2\pi}{D}$. Therefore, each sectorized antenna transmits towards a disk's sector of arc length $\frac{2\pi}{D}$ which reduces the number of active sensors. This technique is commonly referred to as space division multiple access (SDMA). We assume that

the antenna's main lobe gain is given by $G = \frac{D}{1+\gamma(D-1)}$ where $\gamma \in [0,1]$ defines the efficiency of the antenna [10]; the side lobe gain is considered negligible.

2) Ultra-narrow band transmissions: The sensors employ ultra-narrow band transmissions using a random frequency division multiple access (FDMA) scheme [12]. Specifically, the i-th sensor selects a carrier frequency f_i at random from the available bandwidth BW. Let δ be a system parameter, defining the frequency spacing in which collisions occur. Then, if $|f_i - f_j| < \delta$, $i \neq j$, the signals of the i-th and j-th sensor collide [12]. As a result, the collision probability is modeled by $p_c = \delta/BW$.

3) Successive interference cancellation: We assume the reader employs SIC techniques, if the SINR does not achieve the required threshold τ for a certain sensor [13]. Specifically, the reader first attempts to decode and remove the strongest interfering signal. If successful, the reader retries to decode the required signal; otherwise, the process is repeated up to n times during which the reader will either manage to decode the required signal or after the n-th attempt it will be in outage.

IV. Performance Analysis

In this section, we derive the probability of the reader decoding the backscattered signal of a random sensor. The analysis is executed for a typical sensor, denoted by o. Initially, the performance with the two multiple-access schemes, SDMA and FDMA, is considered. We first need the following lemma.

Lemma 1. *The characteristic function of the interference term I in a sensor network of density λ where the nearest interfering signal is at distance ζ, denoted by $\phi_I(t,\lambda,\zeta)$, is given by*

$$\phi_I(t,\lambda,\zeta) = \exp\left\{\pi\lambda\left(\zeta^2 - \xi^2 + \int_0^\infty \Phi(t,h) f_h(h,\rho)\mathrm{d}h\right)\right\}, \tag{7}$$

where $\Phi(t,h)$ is given by

$$\Phi(t,h) = \frac{(-\imath t\beta GPh)^{\frac{1}{\alpha}}}{\alpha}\left(\Gamma\left[-\frac{1}{\alpha}, -\frac{\imath t\beta GPh}{\xi^{2\alpha}}\right] - \Gamma\left[-\frac{1}{\alpha}, -\frac{\imath t\beta GPh}{\zeta^{2\alpha}}\right]\right). \tag{8}$$

Proof: The characteristic function $\phi_I(t,\lambda,\zeta)$ of the interference term $I = \beta GP\sum_{j\in\Psi}\frac{h_j}{d_j^{2\alpha}}$ is given by

$$\begin{aligned}
\phi_I(t,\lambda,\zeta) &= \mathbb{E}\left[\exp\{\imath tI\}\right] \\
&= \mathbb{E}_{\Psi,h_j}\left[\exp\left\{\imath t\beta GP\sum_{j\in\Psi}\frac{h_j}{d_j^{2\alpha}}\right\}\right] \\
&= \exp\left\{2\pi\lambda\int_\zeta^\xi\left(\mathbb{E}_{h_j}\exp\left\{\imath t\beta GP\frac{h_j}{u^{2\alpha}}\right\} - 1\right)u\mathrm{d}u\right\} \quad (9) \\
&= \exp\left\{\pi\lambda\left(\zeta^2 - \xi^2 + \int_0^\infty\int_\zeta^\xi 2\exp\left\{\imath t\beta GP\frac{h}{u^{2\alpha}}\right\}u\mathrm{d}u \times f_h(h,\rho)\mathrm{d}h\right)\right\}, \quad (10)
\end{aligned}$$

where (9) follows from the probability generating functional of a PPP [14], (10) follows by the integral evaluation of u and by unconditioning on h; $f_h(h,\rho)$ is given by either (1) or (2) for $\rho = 0$ and $\rho = 1$, respectively. Then, using the fact $\int_a^b f(x)\mathrm{d}x = \int_0^b f(x)\mathrm{d}x - \int_0^a f(x)\mathrm{d}x$, the final expression can be derived by applying the transformation $v \to -\imath tGP\frac{\beta h}{u^{2\alpha}}$ and the definition of the upper incomplete gamma function [9, 8.350.2]. ∎

We can now state our main theorem.

Theorem 1. *The probability of decoding a random sensor is given by*

$$\Pi_d = \frac{1}{2} - \frac{1}{\alpha\pi(\xi^2-\zeta^2)}\left(\frac{\beta GP}{\tau}\right)^{\frac{1}{\alpha}} \times \int_0^\infty \frac{1}{t}\Im\left[\exp\{\imath t\sigma^2\}(\imath t)^{\frac{1}{\alpha}}\chi(t)\phi_{I_o}(t,\lambda',\zeta)\right]\mathrm{d}t, \tag{11}$$

where $\lambda' = \frac{p_c}{D}\lambda$ and $\chi(t)$ is given by

$$\chi(t) = \int_0^\infty h^{\frac{1}{\alpha}} f_h(h,\rho)\left(\Gamma\left[-\frac{1}{\alpha}, \frac{\imath t\beta GPh}{\tau\xi^{2\alpha}}\right] - \Gamma\left[-\frac{1}{\alpha}, \frac{\imath t\beta GPh}{\tau\zeta^{2\alpha}}\right]\right)\mathrm{d}h, \tag{12}$$

and $\phi_{I_o}(t,\lambda',\zeta)$ is given by Lemma 1.

Proof: The decoding probability of the typical sensor is expressed as $\mathbb{P}(\gamma_o > \tau)$ where τ is a predefined threshold. Therefore, we have

$$\begin{aligned}
\mathbb{P}\left(\frac{G\beta h_o P}{d_o^{2\alpha}(\sigma^2 + I_o)} > \tau\right) &= \mathbb{P}\left(I_o < \frac{\beta GPh_o}{d_o^{2\alpha}\tau} - \sigma^2\right) \\
&= F_{I_o}\left(\frac{\beta GPh_o}{d_o^{2\alpha}\tau} - \sigma^2\right),
\end{aligned}$$

where $F_{I_o}(x)$ is the cumulative distribution function (cdf) of the interference term I_o, which can be evaluated using the Gil-Pelaez inversion theorem [11], that is,

$$F_{I_o}(x) = \frac{1}{2} - \frac{1}{\pi}\int_o^\infty \frac{1}{t}\Im\left[\exp\{-\imath tx\}\phi_{I_o}(t,\lambda,\zeta)\right], \tag{13}$$

where $\phi_{I_o}(t,\lambda,\zeta)$ is the characteristic function of I_o evaluated at t already derived in Lemma 1. Since a sensor interferes with probability p_c and the beamwidth of the reader's sectorized antenna is $2\pi/D$, the density of the interfering sensors is thinned by p_c/D. Therefore, the characteristic function is given by $\phi_{I_o}(t, p_c\lambda/D, \zeta)$. Now we need to derive $\mathbb{E}[\exp\{-\imath tx\}]$ where $x = \frac{\beta GPh_o}{d_o^{2\alpha}\tau} - \sigma^2$. We have

$$\begin{aligned}
\mathbb{E}[\exp\{-\imath tx\}] &= \exp\{\imath t\sigma^2\}\mathbb{E}_{\Psi,h_o}\left[\exp\left\{-\imath t\frac{\beta GPh_o}{d_o^{2\alpha}\tau}\right\}\right] \\
&= \frac{\exp\{\imath t\sigma^2\}}{\pi(\xi^2-\zeta^2)}\int_0^{2\pi}\int_\zeta^\xi \mathbb{E}_{h_o}\left[\exp\left\{-\imath t\frac{\beta GPh_o}{u^{2\alpha}\tau}\right\}\right]u\mathrm{d}u\mathrm{d}\theta,
\end{aligned} \tag{14}$$

which follows by unconditioning on the distance and using (3). Following similar steps to the proof of Lemma 1, the final expression is deduced by some trivial algebraic operations. ∎

We now look at the case where the reader employs SIC. For this case, we consider a fading-free scenario; this is

a reasonable assumption in static environments which are characterized by strong line-of-sight transmissions/receptions. In a fading-free scenario, the order statistics are defined by the distances. In what follows, we use the same notation as above but we drop h where appropriate. We need to derive the decoding probability of the n-th closest sensor as well as the decoding probability of a random sensor after the interfering signal of the n-th sensor has been removed. The required mathematical expressions can be easily deduced from Theorem 1. Specifically, the probability of decoding the n-th closest sensor, denoted by $\mathsf{P_c}^{(n)}$, can be written as

$$\mathsf{P_c}^{(n)} = \frac{1}{2} - \frac{\left(\frac{\beta GP}{\tau}\right)^{\frac{1}{\alpha}}}{2\alpha\pi} \int_0^{\infty} \Im\left[\exp\{\imath t\sigma^2\}(\imath t)^{\frac{1}{\alpha}}\omega(t)\right] \frac{\mathrm{d}t}{t}, \quad (15)$$

with

$$\omega(t) = \int_{\zeta}^{\xi} \exp\left\{-\imath t \frac{\beta GP}{r^{2\alpha}\tau}\right\} \phi_I(t, \lambda', r) f_r(r) \mathrm{d}r, \quad (16)$$

where $\phi_I(t, \lambda', r)$ is given by Lemma 1 and $f_r(r)$ is the pdf of the distance r from the origin to the n-th nearest neighbour, given by [14]

$$f_r(r) = \frac{2(\pi\lambda)^n}{(n-1)!} r^{2n-1} \exp\{-\pi\lambda(r^2 - \zeta^2)\}. \quad (17)$$

Note that (17) is slightly different to the one in [14] as we do not consider distances less than ζ. Similarly, the decoding probability of a random sensor after the n-th interfering signal has been removed, denoted by $\mathsf{P_d}^{(n)}$, is given by (15) but with

$$\omega(t) = \chi(t) \int_{\zeta}^{\xi} \phi_I(t, \lambda', r) f_r(r) \mathrm{d}r, \quad (18)$$

where $\chi(t)$ given by (12). We can now state the following proposition.

Proposition 1. *The probability of decoding a random sensor after attempting to cancel up to n interferers is*

$$\Pi_{\mathrm{SIC}}^{(n)} = \Pi_d + \sum_{i=1}^{n} \left(\prod_{j=0}^{i-1} \left(1 - \mathsf{P_d}^{(j)}\right)\right) \left(\prod_{j=1}^{i} \mathsf{P_c}^{(j)}\right) \mathsf{P_d}^{(i)}, \quad (19)$$

where Π_d is given by Theorem 1 (without fading).

The above proposition is derived by considering the events of the protocol described above and by assuming that these events are independent; this approximation is tight for high thresholds [13]. Note that $\mathsf{P_d}^{(0)} = \Pi_d$, since this is the case where no interfering signal is removed.

Finally, we consider the asymptotic scenario $\lambda \to 0$, i.e. a noise-limited scenario. This refers to scenarios with very small δ which will give $p_c \to 0$ or scenarios with a massive number of sectorized antennas, i.e. $D \to \infty$. This could also be achieved by employing SIC to decode and cancel all interfering signals; however, probabilistically this scenario is not always possible. For the asymptotic case $\lambda \to 0$, we have the following proposition for $\rho = 1$.

Proposition 2. *In a noise-limited scenario and for $\rho = 1$, the decoding probability of a random sensor is given by*

$$\Pi_d^{\lambda \to 0} = \frac{2\left(\frac{\beta GP}{\tau\sigma^2}\right)^{\frac{1}{\alpha}}}{\alpha(\xi^2 - \zeta^2)} \left(\Gamma\left[\frac{2}{\alpha}, \zeta^{\alpha}\sqrt{\frac{\beta GP}{\tau\sigma^2}}\right] - \Gamma\left[\frac{2}{\alpha}, \xi^{\alpha}\sqrt{\frac{\beta GP}{\tau\sigma^2}}\right]\right). \quad (20)$$

Proof: For $\lambda \to 0$, we have $I_o \to 0$, and so the decoding probability is given by

$$\mathbb{P}\left(\frac{\beta GPh_o}{d_o^{2\alpha}\sigma^2} > \tau\right) = \mathbb{P}\left(h_o > \frac{\tau d_o^{2\alpha}\sigma^2}{\beta GP}\right) = \int_0^{2\pi} \int_{\zeta}^{\xi} \exp\left\{-d^{\alpha}\sqrt{\frac{\tau\sigma^2}{\beta GP}}\right\} df_d(d)\mathrm{d}d, \quad (21)$$

which follows from the cdf $F_h(h,1) = \int_0^x f_h(h,1)\mathrm{d}h = 1 - \exp\{-\sqrt{x}\}$ and $f_d(d)$ is given by (3); (20) follows from [9, 3.381]. ∎

The expression for $\rho = 0$ can be derived in a similar way, but it is omitted due to space restrictions.

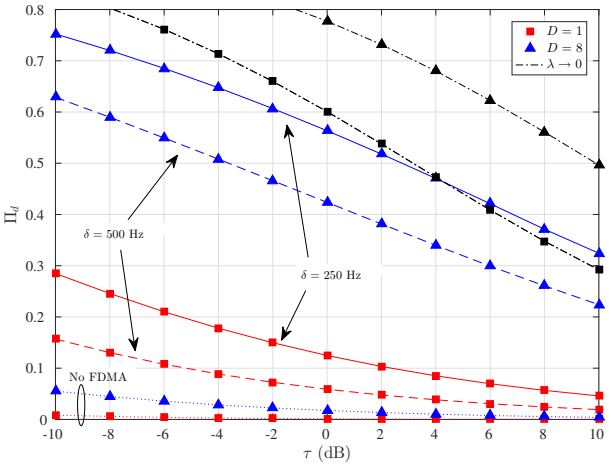

Fig. 2: Decoding probability versus threshold τ; $\lambda = 1$, $\rho = 1$, $P = 20$ dB.

V. Numerical Results

We now validate and evaluate our proposed model with computer simulations. Unless otherwise stated, the simulations use the following parameters: $\lambda = 1$, $\rho = 1$, $P = 20$ dB, $\zeta = 1$ m, $\xi = 10$ m, $\alpha = 2.5$, $\sigma^2 = -30$ dB, $BW = 12$ MHz, $\gamma = 0.1$, $\beta = 0.6$ and $\mu_b = \mu_f = 1$. The lines (dashed or solid) and markers in the plots represent the analytical and simulation results, respectively.

Fig. 2 illustrates the decoding probability with respect to the threshold τ for different values of δ and D. Firstly, it is clear that the decoding probability increases with the employment of the FDMA scheme. Specifically, while δ becomes narrower the decoding probability increases which is expected since the narrower δ is, the smaller the probability of collision becomes. The same behaviour can be observed for the number of sectorized antennas D, that is, the performance increases with D since a smaller sector implies fewer collisions from

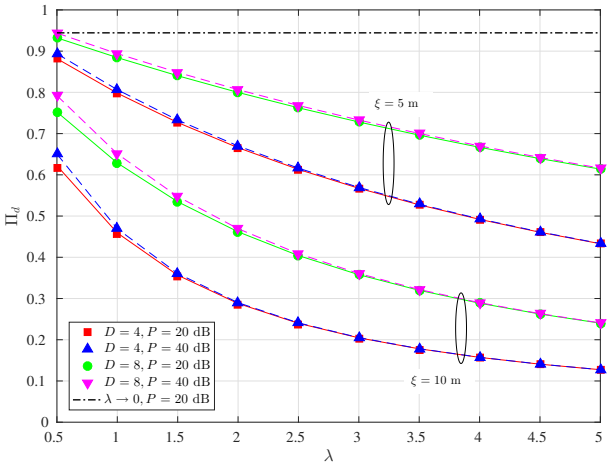

Fig. 3: Decoding probability versus density λ; $\tau = -10$ dB, $\rho = 1$, $\delta = 300$ Hz.

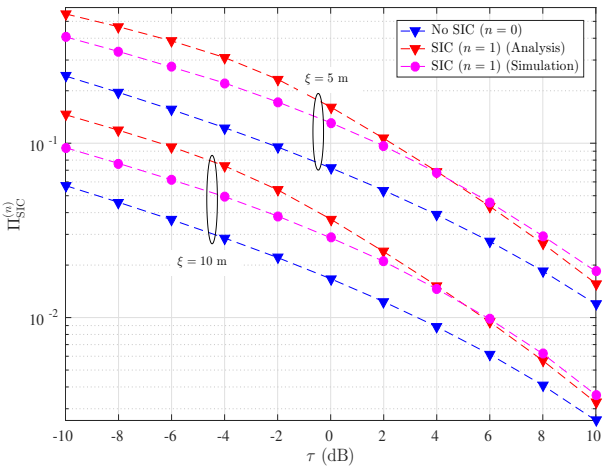

Fig. 4: Decoding probability versus threshold τ with SIC; $\lambda = 1$, $P = 20$ dB, $\rho = 1$, $D = 8$, $n = 1$.

other sensors. It is important to point out how critical δ and D are to the system's performance since, for $D = 1$ and no FDMA, the decoding probability is close to zero. The scenario $\lambda \to 0$ provides high performances as expected. However, for high threshold values, the case $D = 1$, $\lambda \to 0$ is outperformed by $D = 8$, $\lambda = 1$ due to higher antenna gain when $D = 8$. Finally, our theoretical results (lines) perfectly match the simulation results (markers) which validates our analysis. Fig. 3 depicts the decoding probability in terms of the network's density λ for different values of ξ and P. As expected, denser networks provide lower performances due to the existence of more collisions. The same is true for the disk radius ξ, that is, for smaller values of ξ, collisions are reduced since the number of deployed sensors is smaller. Furthermore, the figure shows the effect of the reader's transmit power P to the decoding performance. Increasing P results in an increase to each sensor's backscattered power, which in turn implies an increase to the interference observed at the reader. Therefore, when $\xi = 10$ m, this increase does not provide much gains; indeed, for large λ the performance between $P = 20$ dB and $P = 40$ dB is the same. On the other hand, for $\xi = 5$ m, the gain in performance is more apparent but it's clear that it still decreases for large λ. Finally, Fig. 4 shows the decoding probability when the reader employs SIC. We consider a low-complexity scenario with $n = 1$. As already mentioned, the assumption in Proposition 1 that the events are independent, provides a tight approximation for high threshold values. It's clear from the figure that the employment of SIC provides significant gains to the performance even if just the first nearest sensor is cancelled.

VI. Conclusion

In this paper, we studied backscatter communication sensor networks with spatial randomness. As the reader in such networks suffers from high interference levels due to the multiple concurrent transmissions, we investigated three techniques to reduce the interference and boost the performance: antenna directionality, ultra-narrow band transmissions and SIC at the reader. We derived closed-form expressions for the decoding probability using mathematical tools from stochastic geometry. Our results showed that a combination of these techniques is needed to achieve significant gains. Future extension of this work, is to consider a backscatter multi-cell communication scenario.

References

[1] K. Huang, C. Zhong, and G. Zhu, "Some new research trends in wirelessly powered communications," *IEEE Wireless Commun. Mag.*, pp. 19–27, Apr. 2016.

[2] H. Ju and R. Zhang, "Throughput maximization in wireless powered communication networks," *IEEE Trans. Wireless Commun.*, vol. 13, pp. 418–428, Jan. 2014.

[3] I. Krikidis, S. Timotheou, S. Nikolaou, G. Zheng, D. W. K. Ng, and R. Schober, "Simultaneous wireless information and power transfer in modern communication systems," *IEEE Commun. Mag.*, vol. 52, pp. 104–110, Nov. 2014.

[4] N. C. Karmakar, P. Kalansuriya, R. E. Azim, and R. Koswatta, *Chipless radio frequency identification reader signal processing*, Wiley, 2016.

[5] J. D. Griffin and G. D. Durgin, "Gains for RF Tags using multiple antennas," *IEEE Trans. Ant. Prop.*, vol. 56, pp. 563–570, Feb. 2008.

[6] A. Bletsas, S. Siachalou, and J. N. Sahalos, "Anti-collision backscatter sensor networks," *IEEE Trans. Wireless Commun.*, vol. 8, pp. 5018–5029, Oct. 2009.

[7] A. Bekkali, S. Zou, A. Kadri, M. Crisp, and R. V. Penty, "Performance analysis of passive UHF RFID systems under cascaded fading channels and interference effects," *IEEE Trans. Wireless Commun.*, vol. 14, pp. 1421–1433, Mar. 2015.

[8] K. Han and K. Huang, "Wirelessly powered backscatter communication networks: Modeling, coverage and capacity," *IEEE Trans. Wireless Commun.*, vol. 16, pp. 2548–2561, Apr. 2017.

[9] I. S. Gradshteyn and I. M. Ryzhik, *Table of integrals, series, and products*, Elsevier, 2007.

[10] A. M. Hunter, J. G. Andrews, and S. Weber, "Transmission capacity of ad hoc networks with spatial diversity," *IEEE Trans. Wireless Commun.*, vol. 7, pp. 5058–5071, Dec. 2008.

[11] W. Lu, M. Di Renzo, and T. Q. Duong, "On stochastic geometry analysis and optimization of wireless-powered cellular networks," *Proc. IEEE Global Commun. Conf.*, Atlanta, GA, Dec. 2015.

[12] Y. Mo, M.-T. Do, C. Goursaud, and J.-M. Gorce, "Optimization of the predefined number of replications in a ultra narrow band based IoT network," in *Proc. Wireless Days*, Toulouse, France, Mar. 2016.

[13] C. Psomas and I. Krikidis, "Successive interference cancellation in bipolar ad hoc networks with SWIPT," *IEEE Wireless Commun. Lett.*, vol. 5, pp. 364-367, Apr. 2016.

[14] M. Haenggi, *Stochastic geometry for wireless networks*, Cambridge Uni. Press, 2013.